Received 18 February 2023; accepted 28 February 2023. Date of publication 3 March 2023; date of current version 15 March 2023.

Digital Object Identifier 10.1109/OJAP.2023.3252047

Antenna Array Diversity Evaluation Under Multipath Environments With Digital Beamforming

HUGO RODRIGUES DIAS FILGUEIRAS [1,2] (Associate Member, IEEE), TIAGO HENRIQUE BRANDÃO [1], LUIZ AUGUSTO MELO PEREIRA [1], AND ARISMAR CERQUEIRA SODRÉ JUNIOR [1]

[1] Laboratory WOCA, National Institute of Telecommunications, Minas Gerais 37540-000, Brazil

[2] 5G and Information Security Innovation Unit, VS Telecom, São Paulo 04213-001, Brazil

CORRESPONDING AUTHOR: H. R. D. FILGUEIRAS (e-mail: hugofilgueiras@hotmail.com)

This work was supported in part by RNP with resources from MCTIC through the 6G Mobile Communications Systems Project of the Radiocommunication Reference Center (Centro de Referência em Radiocomunicações - CRR) of the National Institute of Telecommunications (Instituto Nacional de Telecomunicações - Inatel), Brazil, under Grant 01245.020548/2021-07.

ABSTRACT This work proposes a methodology for evaluating the antenna array diversity and resultant radiation pattern from digitally-processed-based beamforming systems. Our approach enables to interpret the advanced antenna systems (AAS) coverage and massive multiple-input multiple output (mMIMO) spatial resolution, by the inspection of the array resultant multiple beams. Particularly, the impact on the mMIMO spatial resolution is conducted as a function of the channel correlation, by means of an exclusively radiofrequency (RF) approach, with the advantage of not considering the system-level features, and using a new figure of merit (Λ factor). The new figure of merit enables to evaluate the antenna array diversity from two- and three-dimensional (2D and 3D) beamforming, by computing the number of lobes with gain higher than a unique element. In the 3D case, the figure of merit is based on a differential calculation, which enables performing an infinitesimal counting of lobes per antenna element beamwidth. Such parameter is initially applied to a theoretical dipole-based array, with the purpose of quantifying the created multiple beams by the overlapped radiation patterns from mMIMO systems. Furthermore, the Λ factor is exploited for analyzing the performance of a 64-element and dual-polarized SICL-based slot antenna array and a 64-element dipole-based antenna prototypes, both previously developed by our research group. Finally, it is demonstrated that the Λ factor increases as diversity increases and dipole-based antenna array could be used as an upper limit, attaining 11.46 lobes/rad.

INDEX TERMS 5G, AAS, antenna array, digital beamforming, figure of merit, massive MIMO and TDD.

I. INTRODUCTION

THE FIFTH generation of mobile communication (5G) has been recently standardized by the 3rd Generation Partnership Project (3GPP) in the two first Releases, Releases 15 [1], [2] and 16 [3], which have been mainly conceived for enhanced mobile broadband (eMBB) communications. Massive multiple-input multiple-output (mMIMO) technique enables increasing channel capacity in a multi-user scenario using digital precoding schemes [4] and is capable of supporting an extreme scattering condition [4]. If each channel between transmitter and receiver is composed of multiple paths, without line-of-sight in an extreme case, and the number of samples is large enough, the Central Limit Theorem [5] is respected. This means each channel might be represented by a Rayleigh distribution in magnitude and uniformly distributed in phase.

Digital mMIMO provides enhanced performance if based on time-division duplexing (TDD) technique, which ensures reliable and fast channel state information (CSI) estimation. Most of past mobile generations (1G to 4G) have applied the frequency division duplexing (FDD) mode, but considering mMIMO applications, it could provide an outdated CSI. The 3GPP Release 15, on the other hand, has already standardized the frequency range 2 (FR2), from 24.25 to 52.6 GHz, a TDD mode of operation [2]. However, in this first implementation, the 5G NR (5G New Radio)

has adopted a switched-beam approach, which is more cost-effective [1], [2], although it does not provide the massive spectral efficiency enhancement expected with the fully-digital mMIMO scheme.

TDD-based digital mMIMO makes use of channel reciprocity for ensuring multipath compensation and enhanced data throughput [6]. Base station (BS) knows the pilot information in the uplink (UL), so the observed differences are related to multipath channel fading. BS estimates the resultant channel phase response and properly compensates it in the downlink (DL), with the purpose of ensuring all multiple paths are constructively combined at the user equipment (UE). No prior assumptions on the propagation environment and no predetermined beams are needed, but CSI is measured at BS by observing UL pilots transmitted by the UEs [6].

Particularly from the antenna point of view, most of the works from literature are concerning the antenna array element design for diverse applications, including beamforming, switched beam and diversity-based mMIMO systems [7], [8], [9], [10], [11], [12], [13], [14], [15], [16]. Considering the last one, each antenna array element provides a different radiation pattern, as a consequence, there are multiple overlapped beams to be digitally processed. This technology is commonly named as advanced antenna systems (AAS), which includes the mMIMO antenna array and precoder [6]. In this implementation, the antenna array resultant radiation pattern is usually not evaluated in the literature. For example, a 2-element array based on a dielectric resonator is presented in [9] and their main concerns were the element design, mutual coupling, envelope correlation coefficient (ECC) and total active reflection coefficient (TARC) reduction. In [10], a wideband printed lens antenna with a flared open edge for multi-beam scanning application at 5G millimeter-wave (mmWaves) band has been proposed. Authors have aimed to fulfill the increased data traffic in mobile communications, by proposing a high-gain (15.4 dBi) and wideband antenna (from 26 to 37 GHz). Our research group has recently reported the development of a dual-band switched beam four-element slotted waveguide antenna array (SWAA) able to simultaneously provide a switchable beam over the 28 and 38 GHz bands [11]. Finally, we have recently published a dual-polarized and 2-GHz bandwidth antenna array with 64 slot-based elements, fed by a substrate-integrated coaxial line (SICL-SAA) for reducing the mutual coupling from fully-digital mMIMO systems [15] and a tri-band antenna for covering both FR1 and FR2, with 80 mm-waves radiating elements aiming at mMIMO systems [16]. Complementarily, other works on MIMO antenna array development from the specialized literature are going to be described in the next Section, entitled "Related Works".

In this context, the current work proposes a new methodology using a novel figure of merit for evaluating the antenna array diversity and resultant radiation pattern from digitally-processed-based beamforming systems. The figure of merit represents a tool to assist antenna array designers for properly understanding its performance under a multipath environment without the need for system-level evaluations. The manuscript main contributions are as follows: *i*) a pioneer evaluation of large-scale AAS resultant radiation pattern from digitally-processed-based beamforming systems, which enables to interpretation of the antenna array coverage and mMIMO spatial resolution by the inspection of the resultant multiple beams. *ii*) an analysis of the mMIMO spatial resolution as a function of the correlation among channels, by using an exclusively radiofrequency (RF) approach, i.e., with the advantage of not considering the system-level features. *iii*) the proposal of a new figure of merit (Λ factor), given in lobes per radians (lobes/rad), for quantifying the created multiple beams by the overlapped radiation patterns from mMIMO systems. *iv*) the Λ factor application in two previously developed mm-waves prototypes from our group, both with 64 elements, published in [15] and [16], and compared to a theoretical dipole-based array. The manuscript is structured in six Sections. Section II discusses the state-of-the-art on antenna arrays for MIMO systems. The unprecedented radiation pattern analysis, including the impact of the channel correlation, is described in Section III. Section IV introduces the Λ factor and presents its calculation method. Section V reports a Λ factor study of case using the aforementioned 64-element antenna array prototypes at 26 GHz. Finally, the conclusions and future works are outlined in Section VI.

II. RELATED WORKS

This section is regarding a literature review on related works of antenna arrays for MIMO systems, mainly focusing on the impact of the array topology or system-level features. For instance, the implementation of a TDD-based 128-element mMIMO system has been conducted by Yang et al. in 2017 [12]. The authors have presented an analytical model, link-level simulation and development of their prototype, composed of 128 printed dipole antennas above a metallic plate, divided into 8 sub-arrays of 16 elements, arranged on a planar array. The main contribution was the achieved 69.12 bit/s/Hz spectral efficiency on a quadrature phase-shift keying (QPSK) modulation, which typically provides 1 bit/s/Hz using a conventional single antenna system.

In [13], Temiz et al. have conducted a study on the impact of antenna array geometry on the indoor mMIMO system performance. Their main goal was identifying an antenna array geometry with reduced mutual coupling and channel correlation. The obtained results have proved the proposed "shifted" antenna array outperformances the conventional uniform arrays in terms of network capacity, due to a lower level of mutual coupling among antenna elements and lower channel correlation.

An additional investigation on the array topology was realized by Aslan et al. in 2021 [14]. Their research has been based on evaluating the element spacing periodicity in order to prove that an aperiodic element distribution

TABLE 1. Literature review on antenna arrays for MIMO systems.

Ref.	Contribution	Application	Performance Figure of merit
[9]	Antenna element design	Low-order MIMO	Mutual coupling, ECC and TARC
[10]	Antenna for multiple-beam	Switched-beam	Input impedance
[11]	Dual-band and four-beam switchable antenna design	Switched-beam	Mutual coupling, ECC and TARC
[12]	Reaching up to 69.12 bit/s/Hz spectral efficiency with QPSK modulation	Digital mMIMO	Spectral efficiency
[13]	Proposing a "shifted" antenna array geometry for decreasing channel correlation	Digital mMIMO	Mutual coupling
[14]	Proposing an aperiodic distribution antenna array for decreasing inter-user interference	Beamforming	Side-lobe level and temperature
[15]	SICL-based feeding network and individual back cavity for reducing mutual coupling	Digital mMIMO	Mutual coupling and ECC
[16]	Tri-band antenna and guiding technique for reducing mutual coupling	Low order MIMO and digital mMIMO	Mutual coupling and ECC
[17]	Mutual Coupling Reduction	Low-order MIMO	Mutual coupling and ECC
[18]	Triple-layer metasurface for reducing mutual coupling	Digital mMIMO	Mutual coupling and ECC
[19]	An embeddable decoupling antenna array	Low-order MIMO	Mutual coupling
This work	Novel analysis method, new figure of merit proposal and application	Digital mMIMO	Λ factor

within an array is potential to increase the system quality of service (QoS) in terms of inter-user interference reduction. The arrays performance has been evaluated in terms of interference among multiple users. As a conclusion, higher-order aperiodic arrays have been shown efficient for mitigating inter-user interference by reducing channel correlation. Table 1 compiles the main contributions and applications from the [9], [10], [11], [12], [13], [14], [15], [16], [17], [18], [19], which also includes the previously discussed papers from the Introduction.

It has been noticed many papers from literature rely on proposing new antenna array elements or array topologies aiming at low mutual coupling, without further investigating the entire antenna array performance in a mMIMO

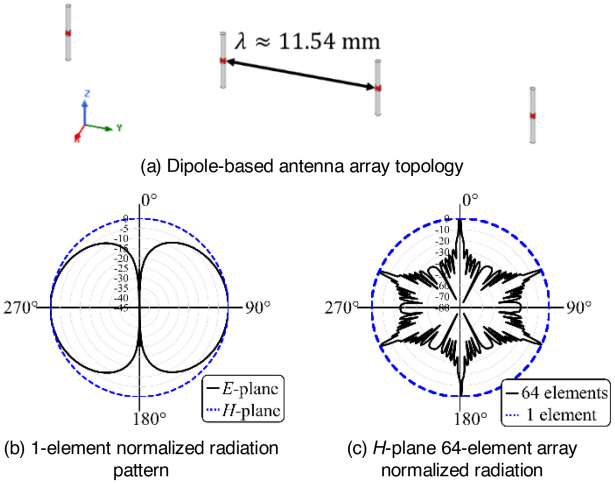

FIGURE 1. 64-element antenna array analysis under a LOS condition.

context. In fact, the antenna array resultant radiation pattern is disregarded in mMIMO applications. Our contribution is regarding the creation of a new figure of merit (Λ factor) for evaluating the resultant large-scale antenna array radiation pattern and its application to a theoretical dipole-based array and the 64-element antenna arrays prototype from [15] and [16]. In other words, most papers propose an antenna array design and use well-known metrics for evaluating it. Our work, in the other hand, is proposing the figure of merit for evaluating any mMIMO antenna array. The drawback of the proposed approach is regarding the current generation of the radiation pattern, which is based on full-wave simulations that could be time-consuming depending on the array order. A possible way to overcome this challenge is by applying the array factor theory for obtaining the resultant radiation pattern for arbitrary magnitude and phase signals.

III. ANTENNA ARRAY RADIATION PATTERN ANALYSIS

It is well known the antenna array elements from TDD-based digital mMIMO systems are independently treated. From the RF point of view, exciting multiple antenna array elements with distinct phase and magnitude will entail a resultant radiation pattern [20], which we intend to evaluate considering different wireless channel scenarios.

We start our evaluation by considering a dipole-based antenna array. Fig. 1(a) presents the array topology of one wavelength (λ)-spaced elements in the magnetic field (*H*)-plane. Fig. 1(b) presents the element radiation pattern in both *H*- and electric field (*E*)-planes, in which we can see an omnidirectional pattern in the *H*-plane as expected. Finally, Fig. 1(c) is related to a 64-element dipole-based array normalized radiation pattern when its elements are excited in phase, i.e., all elements with the same magnitude (1 W) and phase (0°). This radiation pattern would be created if no multipath is considered and a clear line of sight (LOS) is defined between the 64 transmitting antennas and UE. One can note the array capability of creating directive beams pointed to well-defined directions, even though high

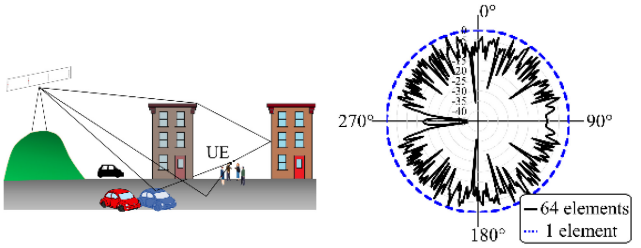

(a) Scenario (b) *H*-plane normalized radiation pattern

FIGURE 2. 64-element analysis under a Rayleigh channel.

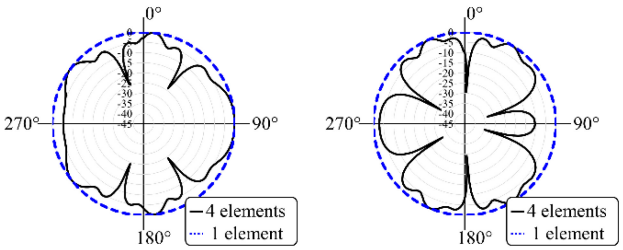

(a) Channel 1 (b) Channel 2

FIGURE 3. Normalized radiation pattern analysis for 4 elements, under the influence of two identically distributed and independent Rayleigh channels.

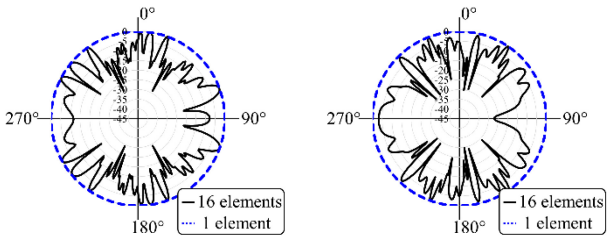

(a) Channel 1 (b) Channel 2

FIGURE 4. Normalized radiation pattern analysis for 16 elements, under the influence of two identically distributed and independent Rayleigh channels.

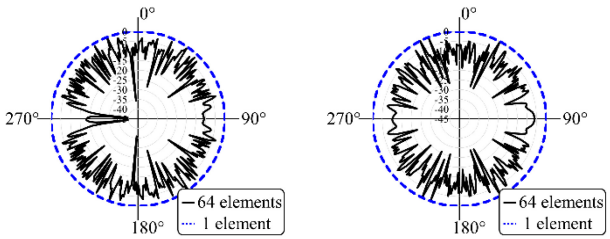

(a) Channel 1 (b) Channel 2

FIGURE 5. Normalized radiation pattern analysis for 64 elements, under the influence of two identically distributed and independent Rayleigh channels.

grating lobes have been created, as expected by the array factor theory [20], since the spacing between adjacent elements is close to λ. It is important to highlight this antenna array has not been designed to operate in this scenario, so its performance is poorer if compared to half-wavelength-spaced phased arrays.

From this point and on, we perform our evaluation in multipath environments. Fig. 2(a) illustrates a multipath scenario under non line of sight (NLOS) conditions. Remembering a TDD-based digital mMIMO system allows compensating each channel response directly in the array element, in such a way we could excite the antenna array with a Rayleigh distributed vector in magnitude and uniformly distributed vector in phase in a worst-case scattering environment. Any other channel could also be applied. Numerically, we could apply this excitation by using the post-processing tool from the full-wave simulator ANSYS HFSS, in which we could stablish the magnitude and phase of each port as desired. We have created arbitrary and completely uncorrelated samples for emulating an uncorrelated channel environment. Fig. 2(b) presents the resultant radiation pattern considering the channel scattering. One can note the antenna array is capable of covering a wider area in the Azimuth plane (H-plane), with maxima and nulls ruled by the channel multipath, when compared to the LOS case from Fig. 1(c). This phenomenon is expected in MIMO systems, since multipath enforces the need for different angles of arrival and departure, thus the antenna array adapts itself to cover a wider area, instead of concentrating the main beam at a unique direction. This feature is deeply confirmed by the evaluation of the array resultant radiation pattern under the influence of channel variation considering 4, 16 and 64 elements. Fig. 3 displays the 4-element array normalized resultant radiation pattern, whereas Fig. 4 and 5 reports the results of the 16- and 64 element antenna arrays, respectively; in all cases compared to the one half-wavelength dipole. Particularly, Fig. 3(a), 4(a) and 5(a) are under the same channel influence, named channel 1, whereas Fig. 3(b), 4(b) and 5(b) are under a second channel influence (channel 2). The difference between the two considered channels is only their generation, maintaining the same statistical parameters ($\sigma = 4$), i.e., two distinct events of the same stochastic process, which could represent two periods with different coherence time.

The analyses of Figs. 3, 4 and 5 allowed us to demonstrate two well-stablished achievements from mMIMO systems, using the proposed methodology: *i*) increasing the number of elements enables to cover the desired area in the *H*-plane with more prominent maxima in the radiation pattern, thus enhancing the mMIMO spatial resolution (as expected by the mMIMO theory), since each mini-lobe has narrower beam; *ii*) by comparing the results of two identically distributed and independent Rayleigh channels, it becomes clear the radiation pattern maxima and nulls are ruled by the wireless channel variations. The latter one implies in radiation pattern adaptation according to the channel, i.e., the RF signal angle of arrival and correspondent excitation for each array element. Differently from the mMIMO theory [4], [6], which typically takes use of capacity and codification features, we innovate by demonstrating the same principles by only evaluating the digitally-beamformed radiation pattern.

We have also evaluated the influence of channel correlation on the antenna array resultant radiation pattern. In this

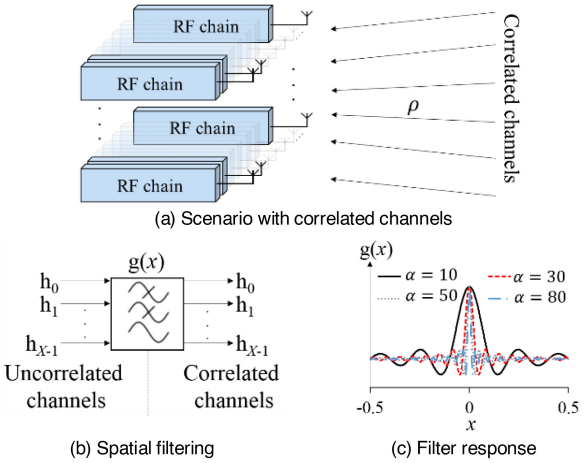

FIGURE 6. The proposed approach to investigate channel correlation influence on the array resultant radiation pattern.

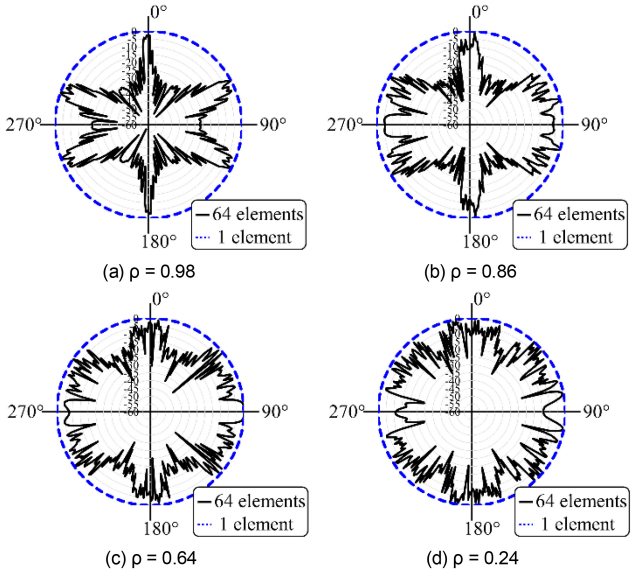

FIGURE 7. Normalized radiation pattern analysis for 64 elements, under the influence of correlated channels as a function of ρ.

TABLE 2. Relation between the filter response and channel correlation for the four evaluated scenarios.

α	ρ
10	0.98
30	0.86
50	0.64
80	0.24

context, we have considered multiple environments, in which the multiple channels between transmitter and receiver have a controlled correlation. Fig. 6(a) describes the proposed scenario with multiple channels correlated by the correlation coefficient ρ, in which each antenna element has its own independently controlled RF chain, as predicted in the mMIMO theory [6], [12], [13], [14], [21], [22]. Each channel correlation is regarded to a specific environment, in which the $\rho = 0$ represents a non-correlated NLOS multi-path environment. Whilst ρ increases, distinct channel correlation scenarios are observed, which implies in reducing the number of paths between transmitter and receiver. The correlation might be managed by implementing a low-pass spatial filtering process [5], as illustrated in Fig. 6(b). This method introduces correlation to adjacent channels, previously non-correlated, for emulating the wireless propagation environment variation. Fig. 6(c) displays the spatial filter impulse response considering four channel scenarios. Therefore, the adjacent channel correlation is managed by the factor α from the spatial filter response: $g(x) = \text{sinc}(\alpha x)$.

We have used MATLAB for implementing a Monte Carlo simulation to estimate ρ between samples from the filtered vector. The algorithm returns a matrix of correlation factors, in which the calculated coefficients, above and below the main diagonal, represent the correlation factor between each pair of adjacent channels. The observed ρ values have been obtained by taking the mean of all adjacent channel pairs. We have chosen four channel scenarios, whose correlation coefficient values are defined in Table 2. As expected, ρ decreases as α increases, in light of the filter response.

Fig. 7 reports the array normalized radiation patterns considering ρ varying from 0.24 to 0.98. Highly correlated channels ($\rho = 0.98$), demonstrated in Fig. 7(a), provide a directive beam at boresight direction, implying less possible paths between BS a UE, due to the linear dependence between the samples. As ρ reduces, it is possible to observe a dynamic change in the radiation pattern, in which Fig. 7(b), 7(c) and 7(d) present a progressive increase in the number of lobes and nulls, enhancing the mMIMO spatial resolution by means of taking advantage of more paths. As a conclusion, we demonstrate that the radiation pattern is highly-dependent on the correlation level of the samples, coming from Fig. 1(c) to 2(b), i.e., completely correlated to uncorrelated channel samples, respectively. This investigation ratifies the need for uncorrelated channels for proper mMIMO operation [21].

IV. NEW FIGURE OF MERIT: THE Λ FACTOR

This Section introduces the concept and initial application of a novel figure of merit, which has been idealized for evaluating antenna array diversity capacity from the antenna array resultant radiation pattern from AAS, i.e., digitally-processed-based beamforming systems. By considering a digital beamforming approach, one might infer the minimum gain contribution from an antenna array is the gain from a single antenna array element. This means any gain lower than the gain from a unique antenna may be resultant from the overlapped secondary lobes and not from a predominant channel path. In this way, we have conceived the Λ factor, by computing the number of lobes with gain higher than the one-element antenna (NL_h) divided by the one-element antenna beamwidth in the analyzed plane ($\phi_{ab\_element}$ or $\theta_{ab\_element}$) in radians. For instance, the Λ factor for the antenna array from last Section (Fig. 1), in which the array elements are

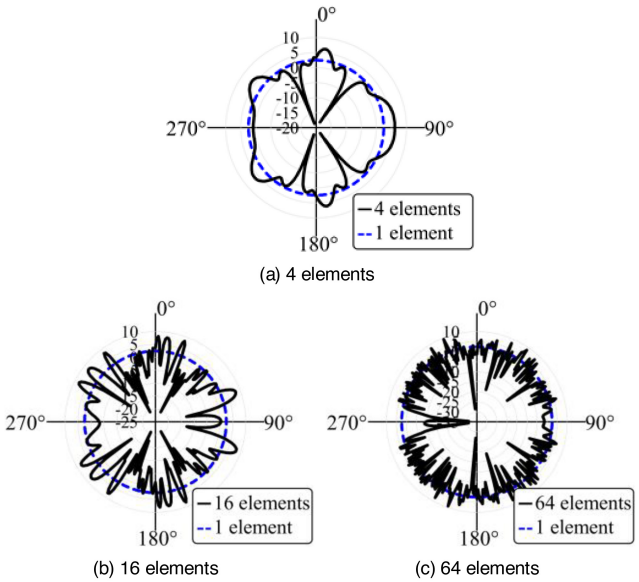

FIGURE 8. Dipole-based antenna array radiation patterns for the Λ factor calculation.

disposed along the y-axis in the H-plane, is given by

$$\Lambda = \frac{NL_{\mathrm{h}}}{\emptyset_{\mathrm{ab\_element}}} [\mathrm{lobes/rad}]. \tag{1}$$

Our initial results were based on two-dimensional beamforming, considering a sectorial and azimuthal coverage, as a proof of concept (Equation (1)). As a progress, a 3D beamforming might be analyzed in a planar array using (2), which uses $\phi_{\mathrm{ab\_element}}$ and $\theta_{\mathrm{ab\_element}}$ as input parameters to calculate Λ. One can note an infinitesimal mean is made in azimuth for counting the number of lobes in the elevation plane (NL_{h}). Finally, the 3D version of Λ is now given in lobes/rad^2 and could be numerically evaluated in future works.

$$\Lambda = \int_{\frac{-\emptyset_{\mathrm{ab_{element}}}}{2}}^{\frac{\emptyset_{\mathrm{ab_{element}}}}{2}} \frac{NL_{\mathrm{h}}(\emptyset)}{\emptyset_{\mathrm{ab_{element}}}\theta_{\mathrm{ab_{element}}}} d\emptyset \tag{2}$$

Fig. 8 presents the radiation pattern from 4, 16 and 64 dipole-based antenna arrays, compared to that of one half-wavelength dipole antenna. We have created a MATLAB code for properly counting the lobes and calculating the proposed figure of merit. From Fig. 8(a), one can observe 05 lobes crossing the radiation pattern from the one half-wavelength dipole, giving rise to $\Lambda = 0.79$ lobes/rad from (1) considering $\phi_{\mathrm{ab\_element}} = 2\pi$. Analogously, there are 24 and 72 lobes with gain higher than one array element in Figs. 8(b) and 8(c), respectively, resulting in $\Lambda = 3.82$ lobes/rad and $\Lambda = 11.46$ lobes/rad for 16 and 64 dipole-based antenna arrays, correspondingly. As a conclusion, the higher is the number of elements, higher is Λ, corroborating with the conclusions made from the analyses of Figs. 3, 4 and 5. Table 3 compiles the achieved results.

We have also evaluated the Λ factor variation in correlated channel environments, using the parameters from Table 2 and the radiation pattern properties from Fig. 9, as reported

TABLE 3. Relation between the array order and λ factor, considering a dipole-based antenna array.

Number of elements	Λ [lobes/rad]
4	0.79
16	3.82
64	11.46

TABLE 4. Relation between the channel correlation and λ factor for the four evaluated scenarios, considering a 64-element dipole-based antenna array.

ρ	Λ [lobes/rad]
0.98	1.91
0.86	4.14
0.64	7.32
0.24	10.50

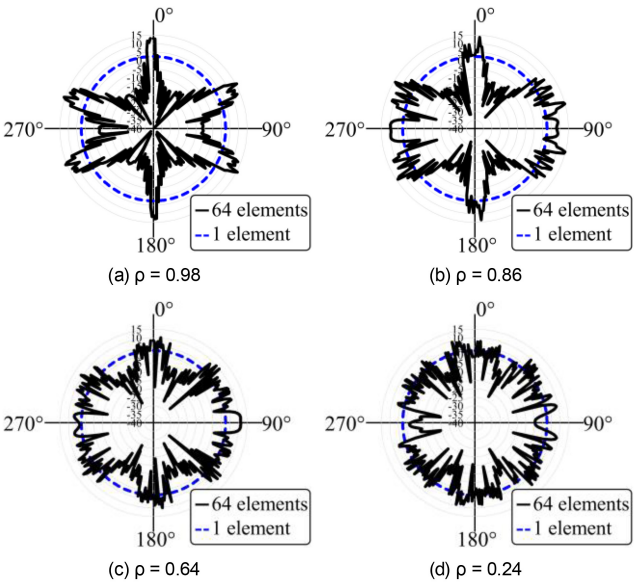

FIGURE 9. Dipole-based antenna array radiation patterns for the Λ factor calculation, considering 64 elements under the influence of correlated channels as a function of ρ.

in Table 4. By managing the correlation among channels, we could not only represent other scenarios, but also express a mutual coupling among elements on a large-scale array. This manuscript only proposes to generically evaluate the correlation impact on the radiation pattern, without specifying the nature of this correlation. One can conclude the Λ factor increases as the correlation among channels decreases, which is also expected, since low channel correlation means a high diversity environment with more lobes for covering diverse paths. Moreover, Fig. 9 shows more crossed beams, when compared to one-element dipole, as the correlation decreases. We have concluded that as the channel correlation increases, our metric decreases. Moreover, one might qualitatively infer an increase in Λ implies in a greater channel capacity, since the channel correlation will be lower [4], [5], [6].

It is important to highlight that the proposed figure of merit could contribute to define the most appropriate array element and/or topology, since it allows to evaluate different antenna arrays performance under the same wireless channel influence. In other words, the Λ factor might be considered potential as the first investigation of a real wireless

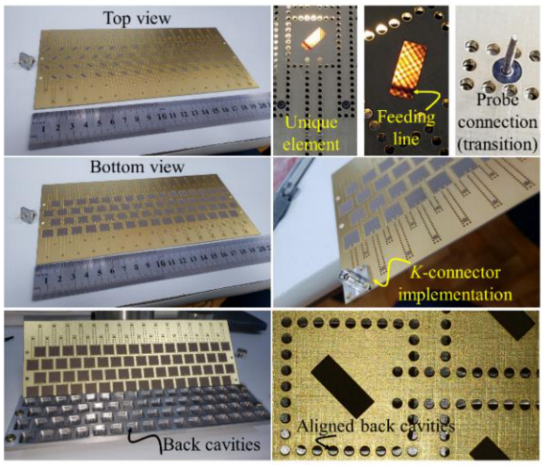

FIGURE 10. The 64-element SICL-SAA prototype.

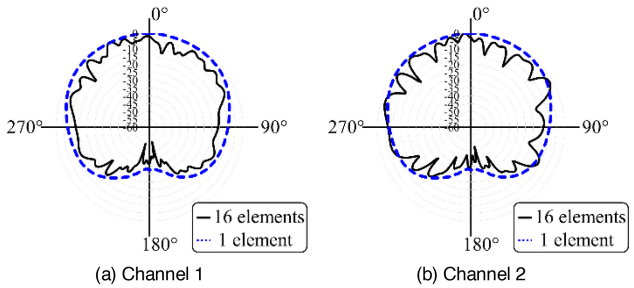

FIGURE 11. Resultant radiation pattern for 16 dual-polarized activated elements.

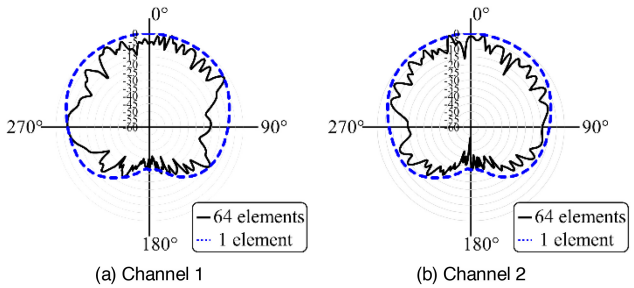

FIGURE 12. Resultant radiation pattern for 64 dual-polarized activated elements.

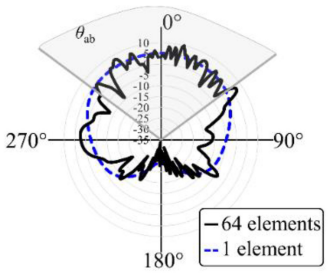

FIGURE 13. SICL-SAA radiation pattern analysis for 64 active elements under the influence of the Channel 1.

deployment for numerically testing diverse radiating elements (patch, slot, dipole or others) and array topologies (linear, squared, triangular, hexagonal, etc) considering the channel distribution. The proposed figure of merit empowers an additional and efficient radiation pattern analysis mechanism for antenna designers from mMIMO systems. Its major advantage is the mentioned professionals do not need to have a background on the system-level features, since our methodology considers only the RF level.

V. STUDY OF CASE USING TWO 64-ELEMENT ANTENNA ARRAY PROTOTYPES

The next step was applying the new figure of merit to a 64-element, slot-based and SICL-fed dual-polarized antenna array (SICL-SAA) prototype (Fig. 10), which has been developed for fully-digital mMIMO applications and described in [15]. It is composed of half-wavelength printed slots with individual three-dimensional back cavities, acting as individual reflectors for ensuring boresight radiation and fed by a SICL feeding line for shielding the propagating mode in the feeding network. The SICL-SAA prototype provides a 2-GHz bandwidth over the lowest range of the 5G NR FR2, around 26 GHz, mutual coupling between adjacent elements lower than −23 dB, 85° beamwidth in both orthogonal planes, 7.4 dBi gain and ECC < 60 dB [15]. All the design procedures were properly discussed and reported in [15]. On the other hand, the current manuscript is focused on applying the Λ factor.

We have computed the Λ factor for two different cases: 16 and 64 activated elements. Fig. 11 reports the 16 dual-polarized active elements resultant radiation pattern, whereas Fig. 12 that of the complete 64 dual-polarized array. In particular, Figs. 11(a) and 12(a) are under the same channel influence (Channel 1 from Section III), as well as Figs. 11(b) and 12(b) are under a second channel influence (Channel 2 from Section III).

One more time, the two achievements from mMIMO systems are proved by applying our radiation pattern analysis to the SICL-SAA, as reported in Figs. 11 and 12. Consequently, this study of case with a 64-element antenna array prototype validates the analysis of the theoretical dipole-based array from Section III. In other words, increasing the mMIMO array number of elements implies in enhancing the radiation pattern maxima and nulls and they are ruled by the channel variations.

The final step was regarding the Λ factor calculation for the SICL-SAA prototype, applying the Channel 1 conditions, as in the dipole array case, and its radiation patterns reported in Fig. 13. By applying (1), it is obtained $\Lambda = 5.99$ lobes/rad for $\theta_{ab\_element} = 85°$. By varying the analyzed coverage, i.e., the considered beamwidth (θ_{ab}), the news values of our figure of merit are displayed in Table 5. One can observe that as θ_{ab} reduces and the antenna array element provides a flatter gain, the Λ factor tends to be to the theoretical value from the dipole analysis, i.e., $\Lambda = 11.46$ lobes/rad for the Channel 1. This behavior indicates that the dipole Λ factor is the upper limit, which is mostly related to the channel variation itself since the element radiation is constant.

TABLE 5. Λ parameter as a function of desired coverage considering the SICL-SAA.

θ_{ab} [°]	Λ [lobes/rad]
122	5.64
85	5.99
40	7.16
20	8.60
10	11.46

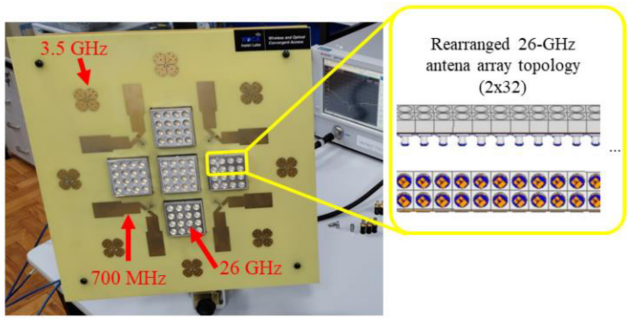

FIGURE 14. The tri-band antenna prototype. Inset presents a zoom-in-view of the numerically rearranged mMIMO antenna for comparison purposes.

TABLE 6. Λ parameter as a function of desired coverage considering the tri-band antenna.

θ_{ab} [°]	Λ [lobes/rad]
122	9.39
85	10.79
40	8.6
20	11.46
10	11.46

The final validation has been made by implementing the proposed metric on a second mm-wave prototype previously published by our group. The prototype is a tri-band antenna for FR1 and FR2 and more details can be found in [16]. A photograph of it is displayed in Fig. 14, in which we can identify 80 26-GHz radiating elements. For a fair comparison, we have numerically rearranged its elements as presented in Fig. 14 inset and investigated 64 activated antennas.

Table 6 presents the achieved results. As a conclusion, we can observe an unexpected result for $\theta_{ab} = 40°$, which can be explained by the fact that we have used only one sample of a stochastic process, i.e., one channel sample. A more precise way to estimate this value should be by means of the mean calculation of multiple channel samples. In any case, the main point of this trial is to observe the tendency to have the dipole value ($\Lambda = 11.46$) as an upper limit as the observed coverage reduces. By comparing both prototypes, it seems that the dipole-based mm-wave antenna modified from [16] is capable of taking advantage of more multipath than the SICL-SAA antenna from [15] since the former's Λ value is comparatively higher, in the analyzed plane. This behavior was in fact expected since this comparison has been made between an array arranged with 16 elements in the analyzed axis (4x16 elements for the SICL-SAA) against 32 elements from the dipole based (2x32 elements). These results reinforce the validity of our proposed metric.

VI. CONCLUSION

This paper presented, for the first time in literature, a methodology for evaluating large-scale antenna arrays from TDD-based fully-digital massive multiple-input multiple-output systems, taking into account the channel response impact on the antenna array radiation pattern. Our methodology differs from the conventional antenna array analysis by evaluating the spatial resolution and diversity performance, exclusively interpreting the digitally-beamformed resultant radiation pattern. Specifically, the proposed approach enables to investigate the impact on the mMIMO spatial resolution as a function of the channel correlation, by simply using a RF approach, with the advantage of not considering the system-level features. In addition, a new figure of merit, named Λ factor, has been created for investigating the performance of the antenna array resultant radiation pattern, which is governed by the array elements phase and magnitude that are defined by the wireless channel response.

The Λ factor has been applied to three different 64-element antenna arrays, namely: a theoretical dipole-based array for properly understanding the array coverage capability under a multipath channel; a dual-polarized SICL-based slotted waveguide antenna array prototype reported by authors in [15]; a tri-band and dipole-based prototype from [16]. It has been proved that as Λ increases, the antenna array becomes capable to cover a wider area, using more prominent and narrow beams, i.e., higher spatial resolution. As a consequence, the higher is the array number of elements, higher the Λ factor is. Additionally, it has been observed the radiation pattern maxima and nulls are ruled by the channel multipath, which means it is constantly adjusted as the wireless channel changes.

The studies-of-case on real prototypes have demonstrated that Λ factor tends to that of the dipole-based antenna array with the same number of elements, under the same wireless channel conditions. The proposed methodology could be considered useful for analyzing the antenna array resultant radiation pattern from TDD-based mMIMO systems. It is a potential solution for evaluating the advantages of using different antenna types as the array elements (crossed dipoles, patches, slots and others) and array topologies for different wireless environments, which could be experimentally validated on system-level experiments. In future works, we envisage applying other distributions for wireless communications and employ an analytical investigation on the array factor theory for reducing the computational effort and further evaluating 3D beamforming. Finally, we intend to mathematically relate the proposed Λ factor to well-known MIMO metrics, such as ECC and ergodic diversity.

ACKNOWLEDGMENT

The authors would like to thank the financial support from RNP, CNPq, CAPES, FINEP and FAPEMIG and the technical support from Prof. Dr. Felipe Augusto Pereira de Figueiredo and Prof. Dr. Rausley Adriano Amaral de Souza, both from Inatel-Brazil.

REFERENCES

[1] *Group Radio Access Network; NR; User Equipment (UE) Radio Transmission and Reception; Part 1: Range 1 Standalone*, 3GPP Standard TS 38.101-1 version 15.5.0 Release 15, Mar. 2019.

[2] *5G; NR; User Equipment (UE) Radio Transmission and Reception; Part 2: Range 2 Standalone*, 3GPP Standard TS 38.101-2 version 15.2.0 Release 15, Sep. 2018.

[3] "3GPP-study on new radio (NR) access technology," 3GPP, Sophia Antipolis, France, 3GPP Rep. TR 38.912 version 16.0.0 Release 16, Sep. 2020.

[4] E. Björnson, E. G. Larsson, and T. L. Marzetta, "Massive MIMO: Ten myths and one critical question," *IEEE Commun. Mag.*, vol. 54, no. 2, pp. 114–123, Feb. 2016.

[5] A. Leon-Garcia, *Probability, Statistics, and Random Processes for Electrical Engineering*, 3rd ed. Upper Saddle River, NJ, USA: Pearson, 2008, pp. 359–410.

[6] J. Ø. Nielsen, A. Karstensen, P. C. F. Eggers, E. De Carvalho, G. Steinböck, and M. Alm, "Precoding for TDD and FDD in measured massive MIMO channels," *IEEE Access*, vol. 8, pp. 193644–193654, 2020.

[7] Y. Yashchyshyn et al., "28 GHz switched-beam antenna based on S-PIN diodes for 5G mobile communications," *IEEE Antennas Wireless Propag. Lett.*, vol. 17, pp. 225–228, 2018.

[8] M. V. Komandla, G. Mishra, and S. K. Sharma, "Investigations on dual slant polarized cavity-backed massive MIMO antenna panel with beamforming," *IEEE Trans. Antennas Propag.*, vol. 65, no. 12, pp. 6794–6799, Dec. 2017.

[9] Y. Zhang, J.-Y. Deng, M.-J. Li, D. Sun, and L.-X. Guo, "A MIMO dielectric resonator antenna with improved isolation for 5G mm-wave applications," *IEEE Antennas Wireless Propag. Lett.*, vol. 18, pp. 747–751, 2019.

[10] M. Xue, W. Wan, Q. Wang, and L. Cao, "Low-profile millimeter-wave broadband metasurface antenna with four resonances," *IEEE Antennas Wireless Propag. Lett.*, vol. 20, pp. 463–467, 2021.

[11] E. C. V. Boas, H. R. D. Filgueiras, I. F. da Costa, J. A. J. Ribeiro, and A. C. Sodre Jr., "Dual-band switched-beam antenna array for MIMO systems," *IET Microw. Antennas Propag.*, vol. 14, no. 1, pp. 82–87, 2020.

[12] X. Yang et al., "Design and implementation of a TDD-based 128-antenna massive MIMO prototype system," *China Commun.*, vol. 14, no. 12, pp. 162–187, Dec. 2017.

[13] M. Temiz, E. Alsusa, L. Danoon, and Y. Zhang, "On the impact of antenna array geometry on indoor wideband massive MIMO networks," *IEEE Trans. Antennas Propag.*, vol. 69, no. 1, pp. 406–416, Jan. 2021.

[14] Y. Aslan, A. Roederer, and A. Yarovoy, "System advantages of using large-scale aperiodic array topologies in future mm-wave 5G/6G base stations: An interdisciplinary look," *IEEE Syst. J.*, vol. 16, no. 1, pp. 1239–1248, Mar. 2022.

[15] H. R. D. Filgueiras and A. C. Sodré Jr., "A 64-element and dual-polarized SICL-based slot antenna array development applied to TDD massive MIMO," *IEEE Antennas Wireless Propag. Lett.*, vol. 21, pp. 750–754, 2022, doi: 10.1109/LAWP.2022.3144916.

[16] T. H. Brandão and A. C. S. Jr., "Tri-band antenna array for FR1/FR2 5G NR base stations," *IEEE Antennas Wireless Propag. Lett.*, early access, Nov. 25, 2022, doi: 10.1109/LAWP.2022.3224827.

[17] M. Elahi, A. Altaf, E. Almajali, and J. Yousaf, "Mutual coupling reduction in closely spaced MIMO dielectric resonator antenna in H-plane using closed metallic loop," *IEEE Access*, vol. 10, pp. 71576–71583, 2022, doi: 10.1109/ACCESS.2022.3187433.

[18] S. Luo, Y. Zhang, G. F. Pedersen, and S. Zhang, "Mutual decoupling for massive MIMO antenna arrays by using triple-layer meta-surface," *IEEE Open J. Antennas Propag.*, vol. 3, pp. 1079–1089, 2022, doi: 10.1109/OJAP.2022.3203252.

[19] Y. Qin, R. Li, and Y. Cui, "Embeddable structure for reducing mutual coupling in massive MIMO antennas," *IEEE Access*, vol. 8, pp. 195102–195112, 2020, doi: 10.1109/ACCESS.2020.3033717.

[20] C. A. Balanis, *Antenna Theory: Analysis and Design*, 3rd ed. Hoboken, NJ, USA: Wiley, 2005, pp. 811–882.

[21] S. Sun, T. S. Rappaport, R. W. Heath, A. Nix, and S. Rangan, "MIMO for millimeter-wave wireless communications: Beamforming, spatial multiplexing, or both?" *IEEE Commun. Mag.*, vol. 52, no. 12, pp. 110–121, Dec. 2014.

[22] "Study on channel model for frequencies from 0.5 to 100 GHz," 3GPP, Sophia Antipolis, France, 3GPP Rep. TR38.901 version 15.0.0 Release 15, 2018.

HUGO RODRIGUES DIAS FILGUEIRAS received the B.Sc., M.Sc., and Ph.D., degrees in telecommunications from the Laboratory Wireless and Optical Convergent Access, National Telecommunications Institute (Inatel). He has acted as a Researcher Engineer of fifth and sixth generation mobile communications networks (5G and 6G) with the Radiocommunications Reference Center, Inatel and a Consultant with the Inatel Competence Center Training and Consulting Team. He acts as an Invited Professor of the Propagation Discipline of Lato Sensu Postgraduate Courses in Network Engineering and Telecommunications Systems with Inatel. He is currently acts as a 5G and Information Security Innovation Manager with VS Telecom, São Paulo. He has more than 30 publications in national and international magazines and conferences of high scientific impact factor and one patent pending. He has teaching experience for being a monitor and a Professor in several subjects of the Telecommunications Engineering Graduation by means of the Teaching Internship Program. He worked on research and development projects in the area of antenna development, analysis of high intensity radiated fields for aeronautical applications and coexistence between IMT and satellite systems. His research interests include the development of antennas, propagation, mobile communication systems, digital modulation schemes, and topologies of optical and wireless access networks stand out.

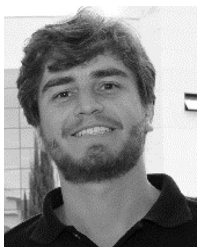

TIAGO HENRIQUE BRANDÃO received the Math degree from UNIVAS, Brazil, in 2009, and the B.Sc. and M.Sc. degrees in telecommunications engineering from Inatel, Brazil, in 2016 and 2019, respectively, where he is currently pursuing the Ph.D. degree in telecommunication. He acted as an Antenna Developer with Ideal Antennas Company from 2018 to 2019. He acts as a Researcher for the Wireless and Optical Convergent Access Laboratory, Inatel. He has experience in teaching for being a Tutor on undergraduate courses with Inatel from 2012 to 2018 in the Teaching Internship Program. His fields of interest are antennas, advanced antenna systems for mobile networks, and mobile networks.

LUIZ AUGUSTO MELO PEREIRA received the B.Sc. and M.Sc. degrees in telecommunications engineering from the National Institute of Telecommunications (Inatel), Brazil, in 2017 and 2020, respectively, where he is currently pursuing the Ph.D. degree in telecommunication. He has experience in teaching for being a Stochastics Process and a Digital Communications II Tutor on undergraduate courses with Inatel from 2018 to 2021 in the Teaching Internship Program. He is currently acts as a Researcher for the Laboratory WOCA, Inatel. His research interests include optical communications, mobile communication systems, wireless systems, microwave photonics, and machine learning-based techniques applied to communication.

ARISMAR CERQUEIRA SODRÉ JUNIOR received the B.Sc. degree in electrical engineering from the Federal University of Bahia, Brazil, in 2001, the M.Sc. degree from the State University of Campinas, Brazil, in 2002, and the Ph.D. degree from Scuola Superiore Sant'Anna, Italy, in 2006. He was an Invited Researcher and a Professor from many world-recognized universities, such as the University of Oulu in 2017, Scuola Superiore Sant'Anna, Italy, in 2015 and 2017, Danish Technical University, Denmark, in 2013, Max-Planck Institute, Germany, in 2010, and the University of Bath, U.K., in 2004, 2005, and 2007.